This is a peer-reviewed, author's accepted manuscript of the following research article: Samende, C., Bhagavathy, S. M., & McCulloch, M. (2022). Power loss minimisation of off-grid solar DC nano-grids - part II: a quasi-consensus-based distributed control algorithm. IEEE Transactions on Smart Grid, 13(1), 38-46. https://doi.org/10.1109/TSG.2021.3111779



# Power Loss Minimisation of Off-Grid Solar DC Nano-Grids—Part II: A Quasi-Consensus Based Distributed Control Algorithm

Cephas Samende, *Student Member, IEEE,* Sivapriya M. Bhagavathy, *Member, IEEE,* and Malcolm McCulloch, *Senior Member, IEEE*

***Abstract*—This paper investigates the power loss minimization problem of solar DC nanogrids that are designed to provide energy access to households in off-grid areas. We consider nano-grids with distributed battery storage energy systems and that are enabled by multi-port DC-DC converters. As the nano-grids are not connected to the national grid and have batteries and converters distributed in each household, addressing the power loss problem while ensuring supply-demand balance is a challenge. To address the challenge, we propose a novel quasi-consensus based distributed control approach. The proposed approach consists of two algorithms namely, incremental loss consensus algorithm and voltage consensus algorithm. The incremental loss consensus algorithm is proposed to optimally schedule the battery charge/discharge operation while ensuring that supply-demand balance and the battery constraints are satisfied. The voltage consensus algorithm is proposed to determine optimal distribution voltage set points which act as optimal control signals. Both algorithms are implemented in a distributed manner, where minimal information exchange between households is required to obtain the optimal control actions. Simulation results of a solar DC nano-grid with five interconnected households verify the effectiveness of the proposed approach at addressing the nano-grid power loss problem.**

***Index Terms*—Energy access, multi-port converter, solar DC nano-grid, power losses, distributed control, battery storage energy system.**

## NOMENCLATURE

| | |
|---|---|
| $R_{dc,i}$ | Distribution line resistance |
| $r_{b,i}$ | Battery's internal resistance at time *t* |
| $v_{dc,i}$ | Distribution voltage at time *t* |
| $V_{dc,i}$ | Constant distribution voltage |
| $V_{dc,n}$ | Nominal distribution voltage |
| $v_{b,i}$ | Battery terminal voltage at time *t* |
| $v_{pv,i}$ | Solar panel terminal voltage at time *t* |
| $v_{L,i}$ | Load terminal voltage at time *t* |
| $v^b_{oc,i}$ | Battery's open circuit voltage at time *t* |
| $v^{dc}_{min,i}$ | Minimum distribution voltage |
| $v^{dc}_{max,i}$ | Maximum distribution voltage |
| $V^b_{n,i}$ | Nominal battery voltage |
| $C_{b,i}$ | Battery capacity |
| $i_{dc,i}$ | Distribution line current at tme *t* |
| $i_{b,i}$ | Battery charge/discharge current at time *t* |
| $I_{b,i}$ | Referred battery charge/discharge current |
| $P_{b,i}$ | Battery power output at time *t* |
| $P_{L,i}$ | Load power at time *t* |
| $P_{pv,i}$ | Solar power at time *t* |
| $P^c_{loss,i}$ | Converter loss at time *t* |
| $P^-_{c,i}$ | Converter's minimum power output |
| $P^+_{c,i}$ | Converter's maximum power output |
| $\Delta t$ | Battery charge/discharge time step |
| $e_\lambda$ | Current convergence factor |
| $e_v$ | Voltage convergence factor |
| $SoC_{0,i}$ | Battery's initial State of Charge (SoC) |
| $SoC_i$ | Battery's SoC at time *t* |
| $SoC_{min,i}$ | Battery's minimum SoC |
| $SoC_{max,i}$ | Battery's maximum SoC |
| $\lambda$ | Lagrange multiplier for equality constraint |
| $\mu_i, \sigma_i$ | Lagrange multipliers for inequality constraints |
| $\eta^{ch}_{b,i}, \eta^{dis}_{b,i}$ | Battery charge and discharge efficiency |
| $\alpha_i, \beta_i, \gamma_i$ | Power loss coefficients |

The authors are with the Department of Engineering Science, Energy and Power Group, University of Oxford, Oxford, UK e-mail: {cephas.samende, sivapriya.mothilalbhagavathy, malcolm.mcculloch} @eng.ox.ac.uk.

## I. INTRODUCTION

THIS paper investigates the power loss minimization problem of solar DC nanogrids that are designed to provide energy access to households in off-grid areas.

The increase in need to provide affordable energy access using renewable energy resources has accelerated the development and deployment of solar DC nano-grids in off-grid communities [1]. Solar DC nano-grids (or simply nano-grids for easy of reference) can be defined as small self-sufficient energy systems which can be scaled-up on demand. Fig. 1 shows a typical architecture of a nano-grid. The primary energy source is the rooftop solar photovoltaic (PV) panels. The batteries act as storage units, storing excess energy from the panels during day-time and supplying any deficit power when there is insufficient power produced from the panels.

Compared to micro-grids and mini-grids which have installed capacities ranging from kilowatts to megawatts, nano-grids have small installed capacities ranging from few watts to kilowatts [2], [3]. Thus, due to their size, nano-grids are cheaper and quicker to install and deploy even in the remotest locations compared to micro-grids, mini-grids and grid extension [4]–[6]. As majority of AC electrical appliances in rural areas such as electronic lighting (fluorescent and LED bulbs), mobile phone chargers, radios, TVs and DC motors (fans, pumps) are DC-compatible, DC nano-grids are preferred to AC nano-grids [7], [8]. Also, DC nano-grids do not have synchronization issues due to absence of frequency compared

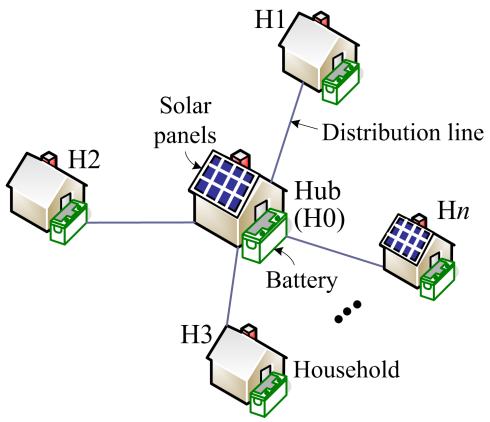


Fig. 1. Diagram of a solar DC nano-grid.

to AC nano-grids. Thus, we consider DC nano-grids in this paper.

Although the nano-grid concept supports the bidirectional exchange of energy between households, offering advantages in terms of increased diversity in power generation and consumption, it also introduces operational, control and technical challenges. Due to lack of a national grid connection, maintaining balance between demand and renewable generation which is intermittent in nature is a challenge. As households in rural areas tend to be far apart from each other, control of the distributed batteries becomes difficult. Power losses which include battery charge and discharge losses, distribution line losses and converter losses are significant in nano-grids deployed in rural areas. The nano-grids can have energy efficiencies as low as 50% especially for distribution voltages less than 120 V [9], which certainly deserves consideration. Thus, to unlock the potential benefits of nano-grids, the above-mentioned challenges must be addressed.

In [5], [10], [11], decentralized voltage control methods are proposed to minimize distribution losses while meeting supply-demand balance in islanded DC micro-grid. Battery and converter losses are however not considered. Also, despite scalability and robustness, decentralized control methods do not guarantee that the locally made decisions can contribute to the global optimal decision of the system. Optimal power flow strategies and heuristic methods such as genetic algorithms are proposed in [12]–[15] to minimize battery, converter and/or distribution line losses of a DC micro-grid. Both strategies are centralized in nature, requiring information from all the households in the nano-grid to make control decisions. This may increase the storage and computational requirements of the controllers, making the whole control system expensive. Greedy algorithms including coalition game theory are proposed in [16]–[19] to minimize distribution line losses in clusters of DC micro-grids. Despite simplicity, greedy algorithms are known to be sub-optimal; their optimality depends on the number of participating micro-grids, i.e. the higher the number of micro-grids, the higher the number of possible coalitions and therefore the lower the power loss [19]. A consensus-based algorithm is proposed in [20] to minimize in a distributed manner the battery losses of a DC micro-grid. Although a distributed approach is considered, converter and distribution line losses are not taken into account. Distribution losses are considered in [21]–[24] without taking battery and converter losses into account. Although several methods have been proposed in the above-mentioned studies, none of them comprehensively considers all the three types of losses namely, battery losses, converter losses and distribution losses in a distributed manner. As ensuring supply-demand balance in a nano-grid is key, accounting for any power loss during nano-grid operation is crucial.

In this paper, a novel quasi-consensus based distributed control algorithm (QCDCA) is proposed to minimize nano-grid battery losses, converter losses and distribution line losses. The proposed algorithm addresses the power loss problem in a distributed manner by finding optimal distribution voltage control signals. It should be noted that this paper is a continuation of our work presented in Part I [25] where the same power loss problem was addressed in a centralized manner. Thus, we adopt the power loss optimization problem formulation described in Part I. The main contributions of this paper are summarized as follows:

- A QCDCA is proposed to address the power loss problem of a multi-port converter enabled nano-grid in a distributed manner. The QCDCA consists of two algorithms namely, incremental loss consensus algorithm (ILCA) and voltage consensus algorithm (VCA).
- The ILCA is proposed to optimally schedule the battery charge/discharge operation while ensuring that supply-demand balance and the battery constraints are satisfied.
- The VCA is proposed to determine optimal distribution voltage set points while ensuring that supply-demand balance is achieved in the distribution network.

The rest of the paper is organised as follows. Section II presents the system model. Section III presents the problem formulation. Section IV presents the proposed control algorithm. Simulation results that verify the performance of the proposed method are given in Section V. Section VI concludes the paper.

## II. System Model

Fig. 1 shows the solar DC nano-grid considered in this paper. It consists of multiple households (labelled H1 to H$n$) that are connected to a central hub (H0) in a spoke and hub manner in order to lower the cost associated with the distribution lines. Four port DC-DC converters (FPCs) are used as multi-port converters to manage the power flow in the nano-grid. The structure of the FPC is shown in Fig. 2.

Each terminal (port) of the FPC is controlled independently without affecting operation of devices connected to other terminals. The load port is controlled to maintain a constant load voltage (e.g. 12 V), since most DC loads in rural areas such as light emitting diode bulbs can operate at constant voltage. The solar port can be independently controlled to either maintain a net zero power injection (in the case of households without solar panels) or operate in maximum power point tracking mode by tracking the appropriate solar panel voltage (if a household/hub has solar panels). The

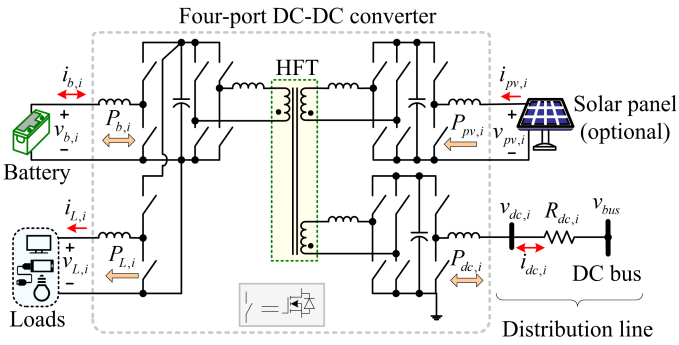


Fig. 2. Integration of the (optional) solar panel, battery, DC loads and distribution line in every household/hub, H*i* of the nano-grid using a FPC.

battery port is not directly regulated and serves as a slack terminal, absorbing and supplying any power imbalance in the network. Power exchange between the hub and households is achieved by regulating the distribution line voltage. This implies that to minimize the power losses in the nano-grid, optimal distribution line voltages should be determined. To formulate and subsequently solve the nano-grid power loss problem, the nano-grid must be modelled first as follows.

### A. Distribution Line Model

Every distribution line connecting a household to the hub is modelled by its resistance, $R_{dc,i}$. In the hub, these distribution lines are connected to a common DC bus bar having voltage, $v_{bus}$ as shown in Fig. 2. The current, $i_{dc,i}$ received by H*i* from the distribution line is calculated as

$$i_{dc,i} = \left(v_{bus} - v_{dc,i}\right)/R_{dc,i} \quad i = 0, 1, \ldots, n \tag{1}$$

Applying Kirchhoff's Current Law (KCL) at the DC bus, $v_{bus}$ can be obtained as

$$v_{bus} = \sum_{i=0}^{n} \frac{v_{dc,i}}{R_{dc,i}} \Big/ \sum_{i=0}^{n} \frac{1}{R_{dc,i}} \tag{2}$$

### B. Solar Panel Model

Solar panels directly convert solar irradiance and temperature into DC power, $P_{pv,i}$ and voltage, $v_{pv,i}$. The solar panel model presented in [26] is used in this paper.

### C. Load Model

We consider constant-power loads such as sewing machines, water pumps, light emitting diode lights, Television sets, radios and cell phone chargers. Other load types which include constant-current loads such as welding machines and constant-impedance loads such as stove tops and water heaters are beyond the scope of this paper. Thus, we model the loads by their load voltage $v_{L,i}$ and load power $P_{L,i}$.

### D. Battery Model

Key properties of a battery are its cell open circuit voltage, $v^b_{oc,i}$, cell internal resistance, $r_{b,i}$ and SoC, $SoC_i$. The $v^b_{oc,i}$ and $r_{b,i}$ are related to $SoC_i$ as given in (3) [12].

$$\begin{cases} v^b_{oc,i} = a_0 e^{-a_1 SoC_i} + a_2 + a_3 SoC_i - a_4 SoC_i^2 + a_5 SoC_i^3 \\ r_s = b_0 e^{-b_1 SoC_i} + b_2 + b_3 SoC_i - b_4 SoC_i^2 + b_5 SoC_i^3 \\ r_{ts} = c_0 e^{-c_1 SoC_i} + c_2\,, \quad r_{tl} = d_0 e^{-d_1 SoC_i} + d_2 \\ r_{b,i} = r_s + r_{ts} + r_{tl} \end{cases} \tag{3}$$

where $a_0, \ldots, a_5$, $b_0, \ldots, b_5$, $c_0, \ldots, c_2$ and $d_0, \ldots, d_2$ are coefficients (of 860 mAh, 3.7 V Lithium-ion battery cell), which are given in [25].

The battery cell current, $i_{cell,i}$ for a given $P_{b,i}$ can be obtained as

$$i_{cell,i} = 0.5 v^b_{oc,i}/r_{b,i} - 0.5\sqrt{\left(v^b_{oc,i}/r_{b,i}\right)^2 - 4P_{b,i}/\left(N_s N_p r_{b,i}\right)} \tag{4}$$

where $N_s = V^b_{n,i}/3.7$ and $N_p = C_{b,i}/0.86$ are numbers of equivalent 860 mAh, 3.7 V Lithium-ion battery cells connected in series and parallel respectively. The $SoC_i$ is estimated in discrete time domain [12] as

$$SoC_i = \begin{cases} SoC_{0,i} - \eta^{ch}_{b,i} P_{b,i} \Delta t / C_{b,i}\,, & P_{b,i} < 0 \\ SoC_{0,i} - P_{b,i} \Delta t / \left(\eta^{dis}_{b,i} C_{b,i}\right)\,, & P_{b,i} \geq 0 \end{cases} \tag{5}$$

The $\eta^{ch}_{b,i}$ and $\eta^{dis}_{b,i}$ can be calculated as

$$\eta^{ch}_{b,i} = v^b_{oc,i}/v_{b,i}\,, \quad \eta^{dis}_{b,i} = v_{b,i}/v^b_{oc,i} \tag{6}$$

where $v_{b,i}$ for a given $P_{b,i}$ can be calculated as

$$v_{b,i} = P_{b,i}/i_{b,i}\,, \quad (i_{b,i} = N_p i_{cell,i}) \tag{7}$$

### E. Four-port DC-DC Converter Model

The structure of the considered FPC is shown in Fig. 2. The key physical phenomenon of the FPC is the power loss which occurs as currents and voltages are converted from one form to another. The FPC loss $p^c_{loss,i}$ can be expressed as a quadratic function of load power, $P_{L,i}$ as follows [25]

$$p^c_{loss,i} = 17.765 + 0.00175 P_{L,i} + 0.000791 P^2_{L,i} \tag{8}$$

### F. Solar DC Nano-Grid Model

As $P_{pv,i}$ and $P_{L,i}$ can be known, and that $p^c_{loss,i}$ is a function of $P_{L,i}$, these can treated as constants at every time instant. Denoting the ratio of $v_{dc,i}$ to $v_{b,i}$ as $n_{b,i}$ in Fig.2, the battery's $v^b_{oc,i}$ and $r_{b,i}$ at the FPC battery port can be moved to the distribution line side of the FPC to form the nano-grid equivalent circuit model as shown in Fig. 3. Here, the (referred) battery output current and power is given as

$$I_{b,i} = i_{b,i}/n_{b,i} \tag{9a}$$

$$P_{b,i} = I_{b,i} v_{dc,i} \tag{9b}$$

The mismatch current, $I_{m,i}$ is the difference between $P_{pv,i}$, $P_{L,i}$ and $p^c_{loss,i}$ as follows

$$I_{m,i} = \left(P_{pv,i} - P_{L,i} - p^c_{loss,i}\right)/v_{dc,i} \tag{10}$$

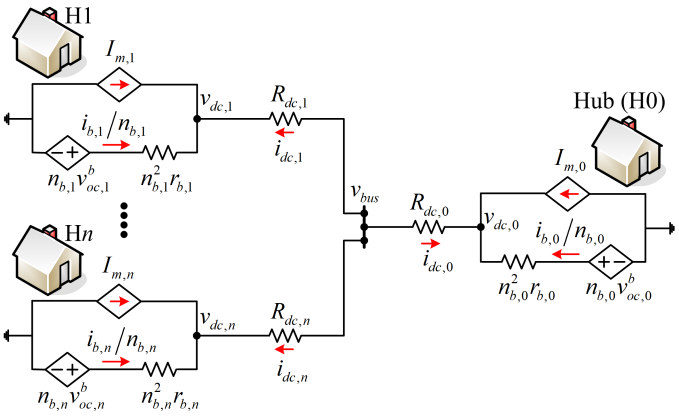


Fig. 3. Equivalent circuit model of a FPC-enabled solar DC nano-grid.

For households without a solar panel, $P_{pv,i} = 0$ in (10). The current, $i_{dc,i}$ received by each H$i$, $i = 0, \ldots, n$ in Fig. 3 must satisfy the KCL as follows

$$i_{dc,i} = -I_{m,i} - I_{b,i} \tag{11}$$

By conservation of current, the algebraic sum of currents, $\Delta I$ in the nano-grid must be equal to zero as follows

$$\Delta I = \sum_{i=0}^{n} i_{dc,i} = \sum_{i=0}^{n} \left(I_{D,i} - I_{b,i}\right) = 0\,, \quad (I_{D,i} = -I_{m,i}) \tag{12}$$

## III. Optimization Problem Formulation

The main objective of this paper is to minimize the total nano-grid power losses, $J$ in a distributed manner. The power losses considered are battery charge and discharge losses, distribution line losses and FPC losses. According to Fig. 3, $J$ can be expressed as

$$J = \sum_{i=0}^{n} \left[\left(-I_{m,i} - I_{b,i}\right)^2 R_{dc,i} + I_{b,i}^2 n_{b,i}^2 r_{b,i} + p^c_{loss,i}\right] \tag{13}$$

To minimize the power losses, the batteries must be optimally dispatched. To achieve this, we adopt a two-step optimization problem formulation approach proposed in our earlier work in [25]. The approach consists of two sub-problems, the optimal battery dispatch problem (OBDP) and the optimal current flow problem (OCFP).

The main objective of the OBDP is to find $\mathbf{I_b} = \left[I^*_{b,0}, \ldots, I^*_{b,n}\right]^T$, a vector of battery charge and discharge currents that minimizes $J$ given by (13) while satisfying some constraints. Using (13) and the expressions developed in Section II, the OBDP can be stated as follows

$$\underset{I_b}{\text{minimize:}} \quad J = \sum_{i=0}^{n} \left(\alpha_i I_{b,i}^2 + \beta_i I_{b,i} + \gamma_i\right) \tag{14a}$$

$$\text{subject to:} \quad \sum_{i=0}^{n} I_{b,i} = \sum_{i=0}^{n} I_{D,i} \tag{14b}$$

$$P^b_{min,i} \le P_{b,i} \le P^b_{max,i} \tag{14c}$$

$$v^{dc}_{min,i} \le v_{dc,i} \le v^{dc}_{max,i} \tag{14d}$$

where

$$\alpha_i = \left(\frac{v_{dc,i}}{v_{b,i}}\right)^2 r_{b,i} + R_{dc,i} \tag{15a}$$

$$\beta_i = \frac{2R_{dc,i}}{v_{dc,i}}\left(P_{pv,i} - P_{L,i} - p^c_{loss,i}\right) \tag{15b}$$

$$\gamma_i = \frac{R_{dc,i}}{v^2_{dc,i}}\left(P_{pv,i} - P_{L,i} - p^c_{loss,i}\right)^2 + p^c_{loss,i} \tag{15c}$$

$$P^b_{max,i} = \min\left(P^+_{c,i}, \frac{\eta^{dis}_{b,i} C_{b,i}\left(SoC_{0,i} - SoC_{min,i}\right)}{\Delta t}\right) \tag{15d}$$

$$P^b_{min,i} = \max\left(P^-_{c,i}, \frac{C_{b,i}\left(SoC_{0,i} - SoC_{max,i}\right)}{\eta^{ch}_{b,i}\Delta t}\right) \tag{15e}$$

Equation (14a) is the objective function of the optimization problem, which in its current form is non-convex due to the non-linear relationship that exists between $v_{dc,i}$, $v_{b,i}$ (which are used to calculate the power loss coefficients; $\alpha_i$, $\beta_i$ and $\gamma_i$ in (15)) and the decision variables, $\mathbf{I_b}$. To convert (14a) to a convex function and (14) to a convex optimization problem thereof, $v_{dc,i}$ and $v_{b,i}$ are treated as constants before each solution iteration and then they get updated for the next solution iteration.

Equation (14b) ensures that currents in the nano-grid are balanced. Inequality (14c) (where $P_{b,i} = I_{b,i}v_{dc,i}$ as given by (9b)) ensures that the battery does not overcharge or over-discharge, which otherwise shortens the lifetime of the battery [27]. It ensures that the minimum SoC, $SoC_{min,i}$, maximum SoC, $SoC_{max,i}$ and converter power limits (i.e. $P^+_{c,i}$ during battery discharging and $P^-_{c,i}$ during battery charging) are satisfied. The second term on the right hand side of equation (15d) places an upper power limit on the battery discharge, and is obtained from (5) for $SoC_i = SoC_{min,i}$. Similarly, a lower power limit is placed on the battery charge through the second term on the right hand side of (15e) for $SoC_i = SoC_{max,i}$.

Lastly, the voltage limits in (14d) ensures that the $v_{dc,i}$ is within the acceptable range where $v^{dc}_{min,i}$ is the lower limit and $v^{dc}_{max,i}$ is the upper limit. In this paper, $v_{dc,i} = V_{dc,i}$ at every iteration to have a convex optimization problem which gets updated at the next iteration.

The main objective of the OCFP is to find distribution voltages, $\mathbf{V_{dc}} = [v_{dc,0}, \ldots, v_{dc,n}]^T$ that corresponds to $\mathbf{I_b}$ obtained from the OBDP (14) by simultaneously solving (1), (2), (10) and (11).

## IV. Proposed Control Algorithm

Fig. 4 shows the schematic diagram of the proposed QCDCA. The proposed algorithm consists of two consensus-based algorithms, ILCA and VCA running sequentially. The ILCA allows the agents to solve the OBDP. The VCA allows the agents to solve the OCFP.

As detailed in Part I of this paper [25], the solution to OBDP (without inequality constraints) can be achieved when the incremental loss $\lambda_i = \partial J/\partial I_{b,i}$ for every $i$-th battery in the nano-grid is equal to the global incremental loss $\lambda$ given by

$$\lambda = \left(\sum_{i=0}^{n} \frac{\beta_i}{2\alpha_i} + \sum_{i=0}^{n} I_{D,i}\right) \Big/ \sum_{i=0}^{n} \left(\frac{1}{2\alpha_i}\right) \tag{16}$$

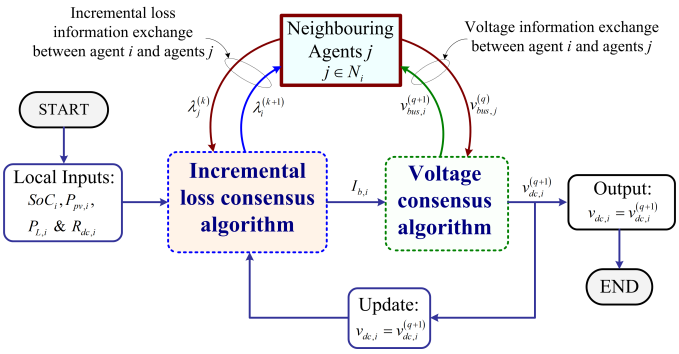


Fig. 4. Schematic diagram of the proposed control algorithm.

The optimal battery charge and discharge current $I^*_{b,i}$ and power $P^*_{b,i}$ for the *i*-th battery can be obtained from (16) as

$$I^*_{b,i} = \frac{\lambda - \beta_i}{2\alpha_i}, \quad P^*_{b,i} = v_{dc,i} I^*_{b,i} \tag{17}$$

Then, taking the constraints given by (14c) into consideration, the optimal $P^*_{b,i}$ can be modified as follows

$$P_{b,i} = \begin{cases} P^*_{b,i}, \text{ if } 0 \le P^*_{b,i} \le P^b_{max,i} \,\&\, SoC_i \ge SoC_{min,i} \\ P^*_{b,i}, \text{ if } P^b_{min,i} \le P^*_{b,i} < 0 \;\&\, SoC_i \le SoC_{max,i} \\ P^b_{max,i}, \text{ if } P^*_{b,i} > P^b_{max,i} \;\&\, SoC_i \ge SoC_{min,i} \\ P^b_{min,i}, \text{ if } P^*_{b,i} < P^b_{min,i} \;\&\, SoC_i \le SoC_{max,i} \\ 0, \text{ otherwise.} \end{cases} \tag{18}$$

The optimal $I^*_{b,i}$ can be modified as

$$I^*_{b,i} = P_{b,i}/v_{dc,i} \tag{19}$$

The solution to OCFP is achieved when: (i) the sum of distribution currents (12) is zero, i.e. $\sum_{i=0}^{n} i_{dc,i} = 0$ and (ii) the bus voltage $v_{bus,i} = v_{dc,i} + i_{dc,i} R_{dc,i}$ estimated from each *i*-th household is equal to $v_{bus}$ expressed in (2).

Thus, by satisfying these two optimality conditions, i.e. $\lambda = \lambda_i$ and $v_{bus} = v_{bus,i}$ for all $i = 0, 1, \ldots, n$, total nano-grid power losses can be minimized. In Part I, these two conditions were satisfied in a centralized manner using a single central controller and two-way communication link between every household and the controller. This has a disadvantage of heavy computational burden on the single controller. To avoid this draw back, the two optimality conditions are achieved in a quasi-distributed manner in this paper. The agents reach consensus on the common $\lambda$ and $v_{bus}$ through exchange of the incremental loss and voltage information with their neighbours.

The ILCA allows the agents to reach consensus on the common $\lambda$, thus solving the OBDP. The VCA allows the agents to reach consensus on the common $v_{bus}$, thus solving the OCFP. To obtain $\Delta I = 0$, one agent, hereafter referred to as a leader agent is chosen to have access to $\Delta I_i$ and $i_{dc,i}$ information from the households. The other *n*-1 agents, hereafter referred to as follower agents do not have to compute for $\Delta I$. Thus, on one hand the leader agent behaves like a centralised controller when accessing the $\Delta I_i$ and $i_{dc,i}$ information from the households while on the other hand, it behaves like a distributed controller when handling the $\lambda = \lambda_i$ and the $v_{bus} = v_{bus,i}$ conditions. For this reason, the proposed algorithm is referred to as quasi and offers advantages of both the centralised and distributed control approaches such as accuracy and low computation burden for large nano-grids.

### A. The Incremental Loss Consensus Algorithm

The main objective of the proposed ILCA is to allow an *i*-th agent to reach consensus on the common $\lambda$ by running the following proposed ILCA

$$\lambda_i^{(k+1)} = \sum_{j=1}^{n} d_{ij} \lambda_j^{(k)} + \epsilon \Delta I^{(k)}, \quad \epsilon \in [0, e_\lambda] \tag{20}$$

where $k$ is the iteration number, $\lambda_i^{(k)}$ is the incremental loss of agent $i$ at $k$-th iteration, $\lambda_i^{(k+1)}$ is the update of $\lambda_i^{(k)}$ with respect to $\lambda_j^{(k)}$ from neighbouring agents $j$, $\Delta I$ is given by (14b), $e_\lambda$ is a small positive number and $d_{ij}$ is the communication gain between agent *i*-and *j* [28], which is expressed as follows

$$d_{ij} = \begin{cases} \frac{2}{d_i + d_j + 1} & \text{if } i \ne j \\ 1 - \sum_{j \in N_i} \left( \frac{2}{d_i + d_j + 1} \right) & \text{if } i = j \\ 0 & \text{otherwise} \end{cases} \tag{21}$$

where $N_i$ is set of neighbours of agent $i$, $d_i$ and $d_j$ are number of neighbouring agents to agent $i$ and agent $j$ respectively.

Since the follower agents do not have to compute for $\Delta I$, substituting $\epsilon = 0$ in (20) represents the ILCA for the follower agents and for the leader agent otherwise. Each agent *i* updates its optimal battery charge/discharge power, $P^*_{b,i}$ and current, $I^*_{b,i}$ at every *k*-th iteration by substituting (20) in (17), (18) and (19). Convergence and optimality of the proposed algorithm was proved as follows. Denoting the leader agent by index 0, convergence of the ILCA (20) is analysed by first rewriting it in matrix form as follows

$$\lambda^{(k+1)} = \mathbf{D} \lambda^{(k)} + \mathbf{E}^{(k)} \tag{22}$$

where $\lambda^{(k)} = \left[ \lambda_0^{(k)}, \ldots, \lambda_n^{(k)} \right]^T$, $\mathbf{E}^{(k)} = [\epsilon \Delta I^{(k)}, 0, \ldots, 0]^T$ and $\mathbf{D} = (d_{ij}) n \times n$ is a doubly stochastic matrix which describes the information exchange on a communication graph [28].

Then, pre-multiplying (22) by $\mathbf{1}^T$ and taking limits as $k \to \infty$ on both sides of (22), the following expression is obtained

$$\lim_{k \to \infty} \mathbf{1}^T \lambda^{(k+1)} = \lim_{k \to \infty} \mathbf{1}^T \mathbf{D} \lambda^{(k)} + \lim_{k \to \infty} \mathbf{1}^T \mathbf{E}^{(k)} \tag{23}$$

Noting that $\mathbf{1}^T \mathbf{D} = 1$ because $\mathbf{D}$ is doubly stochastic and that at equilibrium, $\Delta I = 0$ making $\mathbf{E}^{(k)} = 0$, (23) simplifies to the following expression

$$\lim_{k \to \infty} \mathbf{1}^T \lambda^{(k+1)} = \lim_{k \to \infty} \mathbf{1}^T \lambda^{(k)} \tag{24}$$

That is, as $k \to \infty$, the equal incremental loss principle, $\lambda_i(\infty) = \lambda_j(\infty) = \lambda$ is always achieved and that the ILCA

converges. The ILCA can be initialised using (17) and (14b) as follows

$$\begin{cases} \Delta I^{(0)} = 0 \\ I_{b,i}^{(0)} = I_{D,oi} \\ \lambda_i^{(0)} = 2\alpha_{oi} I_{b,i}^{(0)} + \beta_{oi} \end{cases} \tag{25}$$

To ensure that the ILCA converges regardless of the number of households, the convergence factor $e_\lambda \in [0,1]$ at every iteration $k$ can be updated as $e_\lambda \leftarrow 0.95 e_\lambda$, where 0.95 is a decay factor and $e_\lambda = 1$ at iteration $k = 0$.

### B. The Voltage Consensus Algorithm

The main objective of the proposed VCA is to allow each agent in the nano-grid to reach consensus on the common $v_{bus}$ by running the following proposed VCA

$$v_{bus,i}^{(q+1)} = \sum_{j=0}^{n} \left( d_{ij} v_{bus,j}^{(q)} \right) - \epsilon I_{sum}^{(q)}, \quad \epsilon \in [0, e_v] \tag{26}$$

where $I_{sum} = \sum_{i=0}^{n} i_{dc,i}$, $q$ is the iteration number, $v_{bus,i}^{(q)}$ is the bus voltage estimated by *i*-th agent at $q$, $v_{bus,i}^{(q+1)}$ is the update of $v_{bus,i}^{(q)}$ with respect to $v_{bus,j}^{(q)}$ from neighbouring agents *j*, $d_{ij}$ is given by (21), and $e_v$ is a small positive convergence factor. At every iteration $q$, $e_v \in [0,1]$ can be updated as $e_v \leftarrow 0.95 e_v$, where 0.95 is a decay factor and $e_v$ is initialized as $e_v = 1$.

Similar to the ILCA, substituting $\epsilon = 0$ in (26) represents the VCA for the follower agents and leader agent otherwise. Taking constraint (14d) into account, every agent updates its distribution voltage after every *q*-th iteration as follows

$$v_{dc,i}^{(q+1)} = \begin{cases} v_{bus,i}^{(q+1)} - R_{dc,i} i_{dc,i}, \\ \text{if } v_{min,i}^{dc} \le v_{bus,i}^{(q+1)} - R_{dc,i} i_{dc,i} \le v_{max,i}^{dc} \\ v_{max,i}^{dc}, \text{ if } v_{bus,i}^{(q+1)} - R_{dc,i} i_{dc,i} > v_{max,i}^{dc} \\ v_{min,i}^{dc} \quad \text{otherwise.} \end{cases} \tag{27}$$

Due to the voltage limits in (27), each agent computes a new distribution line current as follows

$$i_{dc,i}^{(q+1)} = \frac{v_{bus,i}^{(q+1)} - v_{dc,i}^{(q+1)}}{R_{dc,i}} \tag{28}$$

Thereafter the leader agent collects the $i_{dc,i}^{(q+1)}$ from the agents to calculate $I_{sum}$. Convergence of the VCA is achieved and the iterations are stopped when $I_{sum} = 0$ or when a pre-defined maximum number of iterations is exceeded.

Similar to the ILCA, denoting the leader agent by index 0, convergence of the VCA is analysed by rewriting (26) in matrix form as follows

$$\mathbf{V_{bus}}^{(q+1)} = \mathbf{D}\mathbf{V_{bus}}^{(q)} + \mathbf{H}^{(q)} \tag{29}$$

where $\mathbf{V_{bus}}^{(q+1)} = \left[ v_{bus,0}^{(q+1)}, \ldots, v_{bus,n}^{(q+1)} \right]^T$, $\mathbf{D} = (d_{ij}) n \times n$ is the doubly stochastic matrix and $\mathbf{H}^{(q)} = [-\epsilon I_{sum}^{(q)}, 0, \ldots, 0]^T$.

Then, pre-multiplying (29) by $\mathbf{1}^T$ and taking limits as $q \to \infty$ on both sides of (29), the following expression is obtained

$$\lim_{q\to\infty} \mathbf{1}^T \mathbf{V_{bus}}^{(q+1)} = \lim_{q\to\infty} \mathbf{1}^T \mathbf{D}\mathbf{V_{bus}}^{(q)} + \lim_{q\to\infty} \mathbf{1}^T \mathbf{H}^{(q)} \tag{30}$$

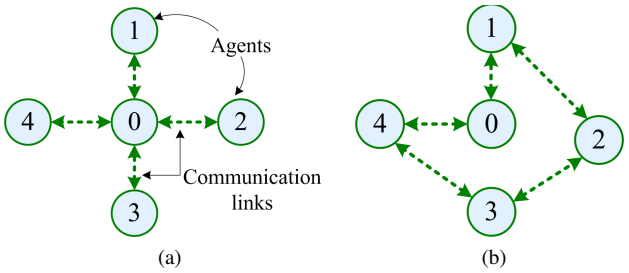


Fig. 5. (a) Star and (b) ring communication graphs for information exchange between the agents. Agents 0, 1, 2, 3, 4 belong to H0, H1, H2, H3 and H4.

Since $\mathbf{1}^T\mathbf{D} = 1$ and that at equilibrium, $I_{sum} = 0$ making $\mathbf{H}^{(q)} = 0$, (30) simplified to the following expression

$$\lim_{q\to\infty} \mathbf{1}^T \mathbf{V_{bus}}^{(q+1)} = \lim_{q\to\infty} \mathbf{1}^T \mathbf{V_{bus}}^{(q)} \tag{31}$$

That is, as $q \to \infty$, all the bus voltages converges as, $v_{bus,i}^{(\infty)} = v_{bus,j}^{(\infty)} = v_{bus}$ for any initial values of the DC bus voltage. Thus, VCA can be initialised as follows

$$\begin{cases} I_{sum}^{(0)} = 0 \\ v_{bus,i}^{(0)} = v_{nom} \end{cases} \tag{32}$$

where $v_{nom}$ is the nominal distribution voltage.

## V. Simulation Results

The performance of the proposed algorithm is tested with a nano-grid which consists of four households ($n = 4$) and a hub as shown in Fig. 1. Battery and line parameters of the nano-grid are given in Table I. FPC simulation parameters are listed in [29]. The $v_{min,i}^{dc}$ and $v_{max,i}^{dc}$ are taken to be 100 V and 120 V, $\forall i = 0, 1, \ldots, n$ respectively. $P_{c,i}^{+}$ and $P_{c,i}^{-}$ are taken to be -120 W and 120 W, $\forall i = 0, 1, \ldots, n$ respectively. The $SoC_{min,i}$ and $SoC_{max,i}$ are 20% and 95%, $\forall, i = 0, 1, \ldots, n$ respectively. The batteries in the households and hub are assumed to have equal initial SoC of 50%. A 2×250 W, 24 V solar panel [30] is used as primary power source at H0.

TABLE I
Battery and Line Parameters.

| | H0 | H1 | H2 | H3 | H4 |
|---|---|---|---|---|---|
| $C_{b,i}$ (kWh) | 0.96 | 1.32 | 2.40 | 1.80 | 1.80 |
| $R_{dc,i}$ (Ω) | 0.01 | 3.0 | 2.0 | 1.5 | 3.0 |
| $V_{dc,n}$ (V) | 110 | 110 | 110 | 110 | 110 |
| $V_{n,i}^{b}$ (V) | 12 | 12 | 12 | 12 | 12 |

### A. Convergence Analysis of ILCA and VCA for Different Communication Graphs

In this section, convergence of the proposed ILCA and VCA is analysed for two different communications graphs: star and ring communication graphs as shown in Fig. 5. The load demands at H0, H1, H2, H3, and H4 are taken to be 74.15 W, 30.171 W, 57.03 W, 57.03 W and 57.03 W respectively. According to (8), the considered load demands give a total

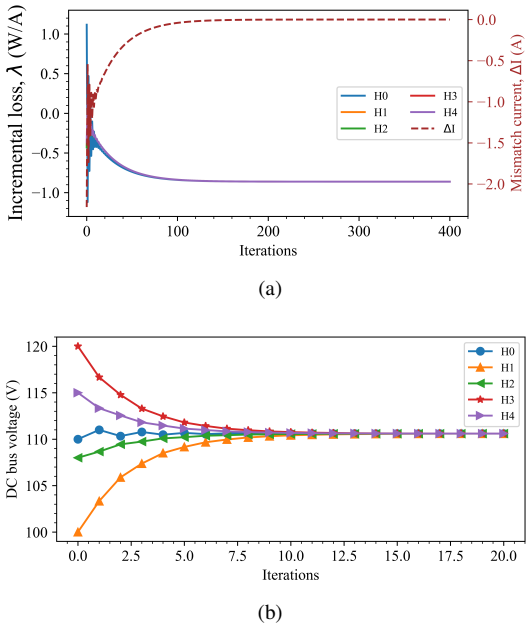


Fig. 6. Convergence speeds of (a) ILCA and (b) VCA for the star communication graph.

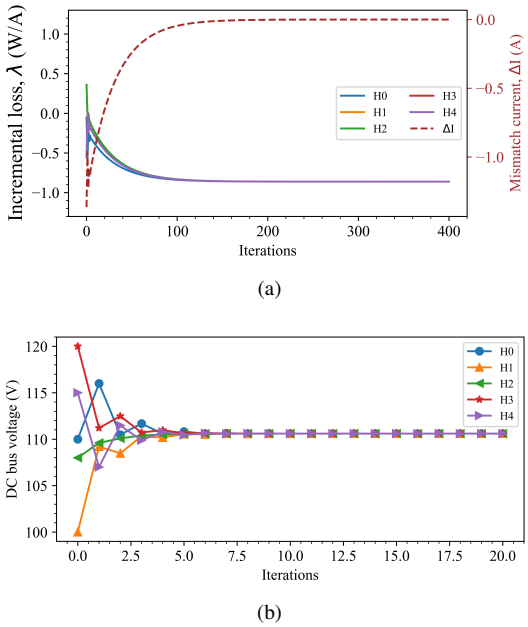


Fig. 7. Convergence speeds of (a) ILCA and (b) VCA for the ring communication graph.

FPC loss of 114.57 W. A power generation of 300 W at H0 is considered so that neither of the batteries are charged nor discharged with absolute maximum power.

Fig. 6 shows that both the ILCA and VCA can converge for the star communication graph. We can observe that at convergence, the supply-demand mismatch current is zero and the household incremental losses stabilise at $\lambda = -0.86$ W/A. It was verified that the obtained $\lambda = -0.86$ W/A is equal to that obtained in centralized manner using (16). Also, the bus voltage converges to 110.6 V after five number of iterations.

Considering the ring communication graph, the results are given in Fig. 7. Comparing Fig. 6 to Fig. 7, we can observe that both algorithms converge to their respective same values. This shows that the proposed algorithm is accurate regardless of the changes in the communication graphs.

### B. Execution Time of the QCDCA

In this section, execution time of the proposed QCDCA for 80 households is presented. The power generation of 500 W at H0 and load demand values considered in the previous case studies are used for simulation. For brevity, the simulation parameters of H4 are duplicated in the extra households, H$i$, $i = 4, 5, \ldots, 80$. The results of the simulation are shown in Fig. 8.

Fig. 8 shows that the execution time increases with the increase in the number of households. For a nano-grid with 80 households, the execution time of the algorithm is less than a minute. As the resolution of solar and demand data is usually more than a minute and that nano-grids in rural areas have less than 80 households, the algorithm is therefore expected to produce control signals in reasonable time.

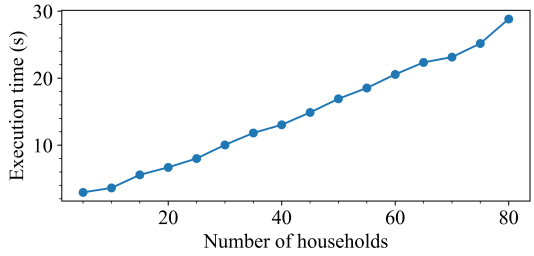


Fig. 8. Variation of the algorithm's execution time with the increase in number of households in a nano-grid.

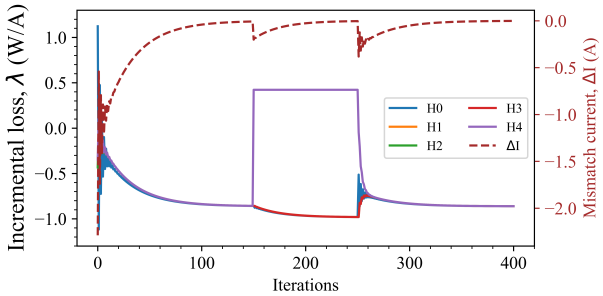


Fig. 9. Plug and play operation of the ILCA.

### C. Performance Analysis of the Proposed algorithm under Plug and Play Operation

Using the ILCA as an example, we show in this section how the ILCA responds to changes in the communication graph due to plug-and-play operation of the system. We use the star communication graph and the simulation parameters used in Section V-A. By disconnecting and connecting H4 back to the system at iteration number 150 and 250 respectively, the results are as shown in Fig. 9.

After disconnecting H4 at 150, the battery in H4 supports its

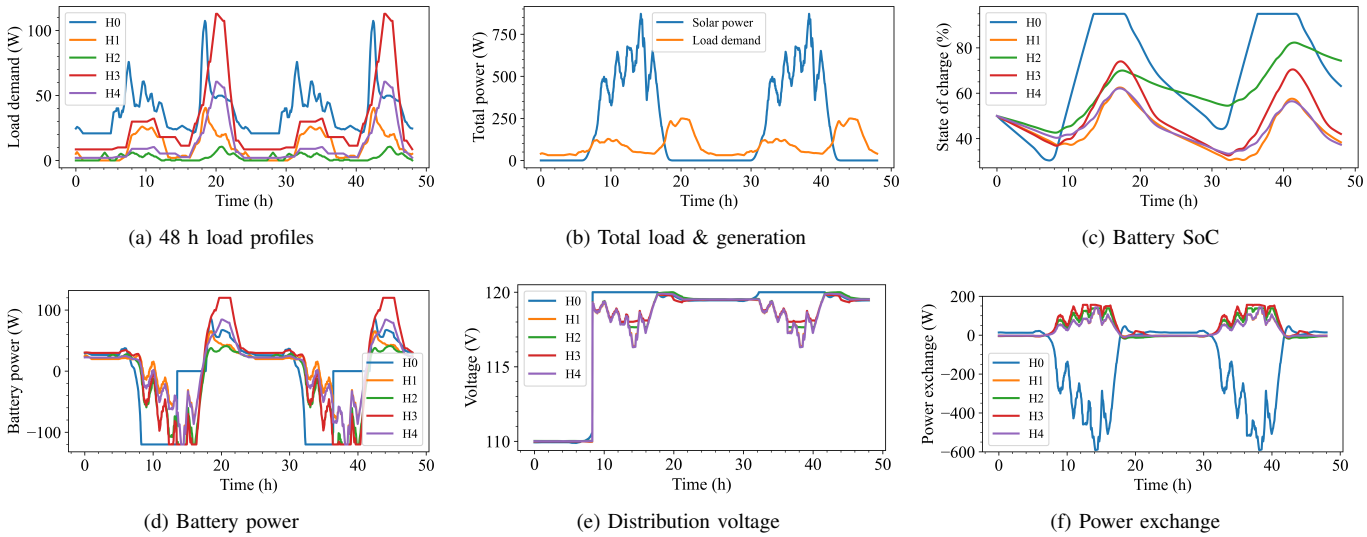


(a) 48 h load profiles (b) Total load & generation (c) Battery SoC

(d) Battery power (e) Distribution voltage (f) Power exchange

Fig. 10. Power management performance of the proposed QCDCA.

local load while the other batteries cooperate to collaboratively support the remaining loads while minimizing the power losses. We can observe that the incremental loss for H4 increases from -0.86 W/A to 0.42 W/A according to (17) to increase the discharge power. The incremental loss for other households except H4 decrease from -0.86 W/A to -0.98 W/A (17), reducing the discharge power. We can also observe that by reconnecting H4 to the system at iteration number 300 that all the incremental losses converge to the initial incremental loss of -0.86 W/A. The supply-demand mismatch current remains at zero throughout the plug-and-play operation. This shows that the proposed algorithm can deal with plug-and-play operations in the nano-grid.

### *D. Power Management Performance of the QCDCA*

In this section, performance of the proposed QCDCA for time varying load demand and solar panel output power is presented. The results are shown in Fig. 10.

We can observe that the proposed algorithm can coordinate the charge and discharge operation of the batteries while keeping the battery output power within $\pm 120$ W and the battery SoC between 20% and 95%. The battery at H0 charges faster than other batteries for most periods because it is situated near the solar panels. Further, we can observe that the batteries charges when PV generation is high and discharge when PV generation is low to meet the total load demand. The proposed algorithm effectively facilitates the power exchange between the households while keeping the voltages within their limits.

## VI. Conclusion

A novel QCDCA is developed in this paper to minimise power losses of multi-port converter enabled solar DC nano-grids. Firstly, a two-stage convex power loss optimization problem consisting of an OBDP and an OCFP is formulated. Then, two consensus-based algorithms, ILCA and VCA, which together form the proposed QCDCA are developed to solve the OBDP and OCFP in a quasi-distributed manner respectively. Simulation results have shown that the proposed algorithm (i) can optimally minimize the power losses while satisfying battery and power balance constraints and (ii) can deal with plug-and-play operations in the nano-grid. The proposed algorithm can be advanced by validating the results through an experiment and investigating the effects of time-delays in the communication networks, and effects of faults in the communication links.

## References

[1] International Energy Agency, "World energy outlook 2019, iea, paris," tech. rep., World Bank, 2019.

[2] H. Kirchhoff and K. Strunz, "Key drivers for successful development of peer-to-peer microgrids for swarm electrification," *Applied Energy*, vol. 244, pp. 46–62, 2019.

[3] P. Hollberg, "Swarm grids-innovation in rural electrification," Master's thesis, 2015.

[4] F. F. Nerini, O. Broad, D. Mentis, M. Welsch, M. Bazilian, and M. Howells, "A cost comparison of technology approaches for improving access to electricity services," *Energy*, vol. 95, pp. 255–265, 2016.

[5] C. Samende, F. Gao, S. M. Bhagavathy, and M. McCulloch, "Decentralized voltage control for efficient power exchange in interconnected dc clusters," *IEEE Transactions on Sustainable Energy*, vol. 12, no. 1, pp. 103–115, 2021.

[6] L. H. P. N. Gunawardena and D. R. Nayanasiri, "Networked DC nanogrid based on multi-port power converters," in *TENCON 2017 - 2017 IEEE Region 10 Conference*, pp. 2727–2732, 2017.

[7] K. Garbesi, V. Vossos, and H. Shen, "Catalog of dc appliances and power systems," tech. rep., Lawrence Berkeley National Lab.(LBNL), Berkeley, CA (United States), 2010.

[8] M. Amin, Y. Arafat, S. Lundberg, and S. Mangold, "Low voltage dc distribution system compared with 230 v ac," in *2011 IEEE Electrical Power and Energy Conference*, pp. 340–345, IEEE, 2011.

[9] M. Nasir, H. A. Khan, A. Hussain, L. Mateen, and N. A. Zaffar, "Solar pv-based scalable dc microgrid for rural electrification in developing regions," *IEEE Transactions on sustainable energy*, vol. 9, no. 1, pp. 390–399, 2017.

[10] C. Ahn and H. Peng, "Decentralized voltage control to minimize distribution power loss of microgrids," *IEEE Transactions on Smart Grid*, vol. 4, no. 3, pp. 1297–1304, 2013.

[11] C. Samende, S. M. Bhagavathy, and M. McCulloch, "State of charge based droop control for coordinated power exchange in low voltage dc nanogrids," in *2019 IEEE 13th International Conference on Power Electronics and Drive Systems (PEDS)*, pp. 1–6, 2019.
[12] T. Morstyn, B. Hredzak, R. P. Aguilera, and V. G. Agelidis, "Model predictive control for distributed microgrid battery energy storage systems," *IEEE Transactions on Control Systems Technology*, vol. 26, no. 3, pp. 1107–1114, 2017.
[13] J. Li, F. Liu, Z. Wang, S. H. Low, and S. Mei, "Optimal power flow in stand-alone dc microgrids," *IEEE Transactions on Power Systems*, vol. 33, no. 5, pp. 5496–5506, 2018.
[14] J.-H. Teng, S.-W. Luan, D.-J. Lee, and Y.-Q. Huang, "Optimal charging/discharging scheduling of battery storage systems for distribution systems interconnected with sizeable pv generation systems," *IEEE Transactions on Power Systems*, vol. 28, no. 2, pp. 1425–1433, 2012.
[15] M. Farasat and A. Arabali, "Voltage and power control for minimising converter and distribution losses in autonomous microgrids," *IET Generation, Transmission & Distribution*, vol. 9, no. 13, pp. 1614–1620, 2015.
[16] F. Mangiatordi, E. Pallotti, D. Panzieri, and L. Capodiferro, "Multi agent system for cooperative energy management in microgrids," in *2016 IEEE 16th International Conference on Environment and Electrical Engineering (EEEIC)*, pp. 1–5, IEEE, 2016.
[17] C. Wei, Z. M. Fadlullah, N. Kato, and I. Stojmenovic, "On optimally reducing power loss in micro-grids with power storage devices," *IEEE Journal on Selected Areas in Communications*, vol. 32, no. 7, pp. 1361–1370, 2014.
[18] T. Zhu, Z. Huang, A. Sharma, J. Su, D. Irwin, A. Mishra, D. Menasche, and P. Shenoy, "Sharing renewable energy in smart microgrids," in *2013 ACM/IEEE International Conference on Cyber-Physical Systems (ICCPS)*, pp. 219–228, IEEE, 2013.
[19] W. Saad, Z. Han, and H. V. Poor, "Coalitional game theory for cooperative micro-grid distribution networks," in *2011 IEEE international conference on communications workshops (ICC)*, pp. 1–5, IEEE, 2011.
[20] Y. Xu, W. Zhang, G. Hug, S. Kar, and Z. Li, "Cooperative control of distributed energy storage systems in a microgrid," *IEEE Transactions on smart grid*, vol. 6, no. 1, pp. 238–248, 2014.
[21] Z. Wang, F. Liu, Y. Chen, S. H. Low, and S. Mei, "Unified distributed control of stand-alone dc microgrids," *IEEE Transactions on Smart Grid*, vol. 10, no. 1, pp. 1013–1024, 2017.
[22] C. Zhao, J. He, P. Cheng, and J. Chen, "Consensus-based energy management in smart grid with transmission losses and directed communication," *IEEE Transactions on smart grid*, vol. 8, no. 5, pp. 2049–2061, 2016.
[23] G. Binetti, A. Davoudi, F. L. Lewis, D. Naso, and B. Turchiano, "Distributed consensus-based economic dispatch with transmission losses," *IEEE Transactions on Power Systems*, vol. 29, no. 4, pp. 1711–1720, 2014.
[24] N. Liu and J. Wang, "Energy sharing for interconnected microgrids with a battery storage system and renewable energy sources based on the alternating direction method of multipliers," *Applied Sciences*, vol. 8, no. 4, p. 590, 2018.
[25] C. Samende, S. M. Bhagavathy, and M. McCulloch, "Power loss minimisation of off-grid solar dc nano-grids—Part I: Centralised control algorithm," *IEEE Transactions on Smart Grid*, 2020.
[26] L. Cristaldi, M. Faifer, M. Rossi, and S. Toscani, "An improved model-based maximum power point tracker for photovoltaic panels," *IEEE Transactions on Instrumentation and Measurement*, vol. 63, no. 1, pp. 63–71, 2013.
[27] Y. Saito, M. Shikano, and H. Kobayashi, "Heat generation behavior during charging and discharging of lithium-ion batteries after long-time storage," *Journal of Power Sources*, vol. 244, pp. 294–299, 2013.
[28] Y. Xu and W. Liu, "Novel multiagent based load restoration algorithm for microgrids," *IEEE Transactions on Smart Grid*, vol. 2, no. 1, pp. 152–161, 2011.
[29] C. Samende, N. Mugwisi, D. J. Rogers, E. Chatzinikolaou, F. Gao, and M. McCulloch, "Power loss analysis of a multiport DC–DC converter for dc grid applications," in *IECON 2018-44th Annual Conference of the IEEE Industrial Electronics Society*, pp. 1412–1417, IEEE, 2018.
[30] Suntech, "250 W monocrystalline solar module," 2012.

**Cephas Samende (M'17)** received the B.Eng. degree in electrical and electronics engineering from the University of Zambia, Lusaka, Zambia in 2014. In 2016, he joined the University of Oxford, Oxford, U.K, where he is currently pursuing a DPhil degree in Engineering Science in the Energy and Power Group, Department of Engineering Science. His current research interests include modelling and control of power electronics, intelligent control and optimization of networked energy systems, application of machine learning and artificial intelligence to local energy markets.

**Sivapriya M. Bhagavathy (M'12)** received the B.Tech. degree in electrical and electronics engineering from the University of Kerala in 2006, M.Tech. in energy systems engineering from Indian Institute of Technology, Bombay and the Ph.D. degree in electrical engineering from the Northumbria University in 2018. She is an Oxford Policy Engagement Network Knowledge Exchange Fellow with the Department of Engineering Science at the University of Oxford, and is a fellow with the Oxford Martin Programme on integrating renewable energy. Her research interests include bridging the gap in energy technology and energy policy, distributed generation and its grid integration, whole system perspective of energy analysis, demand side response using domestic thermal and chemical/electrical storage, electric vehicles as load/storage and electric vehicle infrastructure requirement analysis.

**Malcolm McCulloch (SM'89)** received the B.Sc. (Eng.) and Ph.D. degrees in electrical engineering from the University of the Witwatersrand, Johannesburg, South Africa, in 1986 and 1990, respectively. In 1993, he joined the University of Oxford, Oxford, U.K., to head up the Energy and Power Group, where he is currently an Associate Professor in the Department of Engineering Science. He is active in the areas of electrical machines, transport, and smart grids. His work addresses transforming existing power networks, designing new power networks for the developing world, developing new technology for electric vehicles, and developing approaches to integrated mobility.